



sodium silicate to sodium hydroxide ratio and fly ash to alkaline solution ratio on the compressive strength of fly ash-based geopolymers was assessed using ANNs in [19]. Studies including the prediction of compressive strength of cement-based materials and geopolymer composites using ANNs are [20, 21].

In this study, ANNs are used to determine the compressive strength of geopolymer fly ash. Parameters such as NaOH molarity,  $\text{Na}_2\text{SiO}_3/\text{NaOH}$  ratio, fly ash/alkaline solution ratio, curing temperature, and curing time influence the compressive strength of geopolymer fly ash. Parameter optimization is conducted using ANNs.

## II. EXPERIMENTAL PHASE

### A. Materials

Fly ash, sodium hydroxide (NaOH), and sodium silicate ( $\text{Na}_2\text{SiO}_3$ ) solutions were used. The fly ash was collected from Mettur Thermal power plant, Tamilnadu, India and industrial grade chemicals  $\text{Na}_2\text{SiO}_3$  and NaOH pellets were collected from coimbatore, Tamilnadu. The fly ash was class-F based on its chemical composition [22]. The specific gravity of fly ash was determined in accordance with IS1727 [23] and the value 2.12 was obtained. The chemical composition of  $\text{Na}_2\text{SiO}_3$  solution used is  $\text{SiO}_2=32.2\%$ ,  $\text{Na}_2\text{O}=14.01\%$  and  $\text{H}_2\text{O}=53.79\%$  by mass.



Fig. 1. Geopolymer fly ash cubes.

### B. Sample Preparation and Testing

Sodium hydroxide solution and sodium silicate solution were mixed to prepare the alkaline solution. The alkaline solution was prepared one day before it was mixed with fly ash. Fly ash and alkaline solution were mixed and Geopolymer Fly ash (GF) cubes of  $70.6\text{mm}\times 70.6\text{mm}\times 70.6\text{mm}$  were cast. The GF cubes were subjected to oven curing and were demolded. The compressive strength was tested after one day by keeping the cube specimens at room temperature. Figure 1 shows the Geopolymer Fly ash cubes ready for testing. The five considered parameters and their values are:

- Curing temperature:  $50^\circ\text{C}$ ,  $75^\circ\text{C}$ ,  $100^\circ\text{C}$ ,  $125^\circ\text{C}$ ,  $150^\circ\text{C}$
- Curing time: 1hr, 2hr, 3hr
- Fly Ash/Alkaline Solution ratio (FA/AS): 2.5, 3, 3.5, 4
- $\text{Na}_2\text{SiO}_3/\text{NaOH}$  ratio: 1, 1.5, 2, 2.5
- Molarity of NaOH: 6M, 8M, 10M, 12M

## III. MODELING PHASE

ANNs are used in this study to predict the compressive strength of GF.

### A. Artificial Neural Networks

ANNs are a widely employed method in different fields of artificial intelligence [24]. ANNs are powerful machine learning methods for predicting and solving different scientific computations [16]. ANNs are widely used in the area of civil engineering for predicting concrete's mechanical properties. ANN modeling consists of two steps: 1) Network training with the available training data set and 2) the trained network is tested to compute the prediction accuracy.

### B. Neural Network Model

A Back Propagation Network (BPN) was used in this study to train the ANN model. The BPN training set consists of two stages, the feed forward stage and the back propagation stage. In the feed forward stage, the input node is transferred by the input layer neurons to hidden layer neurons. Each hidden layer neuron calculates the weighted sum of its input, and the sum is transferred through its activation function and the activation value is given to the output layer. The output layer neurons compute the weighted sum of each neuron and the sum is transferred through its activation function, forming the network output value. The sigmoidal function is generally used as activation function. The output is given by:

$$f_j = \frac{1}{1 + \exp\left(-\sum w_{ji}o_i + b\right)} \quad (3)$$

where:  $w_{ji}$  is the connection weight from the lower layer neuron  $i$  to the upper layer neuron  $j$ ,  $o_i$  is the output of the neuron  $i$ , and  $b$  is the bias value. In the second stage, the output layer transfers the network error to the input layer, and the network error is minimized to an acceptable level by adjusting the weights.

The utilized network consists of 5 neurons in the input layer, 5 neurons in the hidden layer, and 1 neuron in the output layer. The hidden neurons are arranged in 2 hidden layers to reduce the error percentage. Table I lists the ANN model parameters. The input layer consists of curing temperature, curing time, fly ash to alkaline solution ratio, sodium silicate to sodium hydroxide ratio, and NaOH molarity and the output layer represents the Compressive Strength (CS) of GF. The data set for preparing ANN model includes 63 experimental results provided in Table II. The ANN prediction accuracy is validated using 66% of the data for training and the remaining data for testing.

TABLE I. ANN MODEL PARAMETERS

Parameter	Value
Number of inputs	5
Number of hidden layers	3
Number of hidden layer units	8
Number of outputs	1
Network architecture	BPN
Training function	Sigmoidal function
Number of training	62
Number of testing	21

TABLE II. ONE DAY CS TEST RESULTS FOR GF CUBES

Sample No	Curing temperature (°C)	Curing time (hr)	FA/AS	Na <sub>2</sub> SiO <sub>3</sub> /NaOH	NaOH molarity	CS (N/mm <sup>2</sup> )
1	50	1	3	2	10	0
2	50	2	3	2	10	0
3	50	3	3	2	10	0.71
4	100	1	3	2	10	4.50
5	100	2	3	2	10	25.08
6	100	3	3	2	10	24.28
7	150	1	3	2	10	7.50
8	150	2	3	2	10	21.16
9	150	3	3	2	10	0
10	100	2	2.5	2	10	6.76
11	100	2	3	2	10	25.08
12	100	2	3.5	2	10	22.28
13	100	2	4	2	10	11.33
14	100	2	3	1	10	28.25
15	100	2	3	1.5	10	31.47
16	100	2	3	2	10	25.08
17	100	2	3	2.5	10	17.48
18	100	2	3	1	8	14.64
19	100	2	3	1.5	8	23.43
20	100	2	3	2	8	17.19
21	100	2	3	2.5	8	14.10
22	100	2	3	1	12	22.07
23	100	2	3	1.5	12	28.44
24	100	2	3	2	12	25.46
25	100	2	3	2.5	12	22.21
26	50	1	3	1.5	10	0
27	50	2	3	1.5	10	0
28	50	3	3	1.5	10	2.95
29	100	1	3	1.5	10	2.90
30	100	2	3	1.5	10	31.47
31	100	3	3	1.5	10	30.27
32	150	1	3	1.5	10	9.71
33	150	2	3	1.5	10	26.22
34	150	3	3	1.5	10	0
35	100	2	2.5	1.5	10	13.09
36	100	2	3	1.5	10	31.47
37	100	2	3.5	1.5	10	30.29
38	100	2	4	1.5	10	20.02
39	75	2	3.5	1.5	12	5
40	100	2	3.5	1.5	12	26.4
41	125	2	3.5	1.5	12	32
42	150	2	3.5	1.5	12	30.5
43	125	1	3.5	1.5	12	16.7
44	125	2	3.5	1.5	12	27.1
45	125	3	3.5	1.5	12	26.2
46	125	2	3.5	1	12	17.5
47	125	2	3.5	1.5	12	21.5
48	125	2	3.5	2	12	20.2
49	125	2	3.5	2.5	12	16.8
50	100	2	1	3	6	25.9
51	100	2	1.5	3	6	23
52	100	2	2	3	6	18.33
53	100	2	2.5	3	6	11.59
54	100	1	1	3	8	2.2
55	100	1	1.5	3	8	9.1
56	100	1	2	3	8	4.2
57	100	1	2.5	3	8	3.8
58	100	1	1	3	10	11.5
59	100	1	2.5	3	10	4
60	100	1	1	3	12	11.8
61	100	1	1.5	3	12	9.5
62	100	1	2	3	12	3.8
63	100	1	2.5	3	12	3

IV. RESULTS AND DISCUSSION

A. Test Results

1) One Day Compressive Strength

The CS of the GF cubes was determined by following the ASTM C109 [25]. The one day compressive strength of 10M GF with different curing temperatures and curing times was obtained as shown in Figure 2. The GF cubes after 1 and 2hr of curing time at 50°C curing temperature were observed in wet condition and no strength was obtained. The strength was increased with rise in temperature and the maximum compressive strength of GF was observed for 100°C curing temperature. Similar results were reported in [26-28]. When the curing temperature became more than 100°C, a gradual decrease in strength was noticed. The curing time also showed influence on compressive strength and the maximum strength was observed for 2hrs curing time. Hence, the maximum value of 31.47N/mm<sup>2</sup> of strength was obtained for 100°C and 2hr curing time.

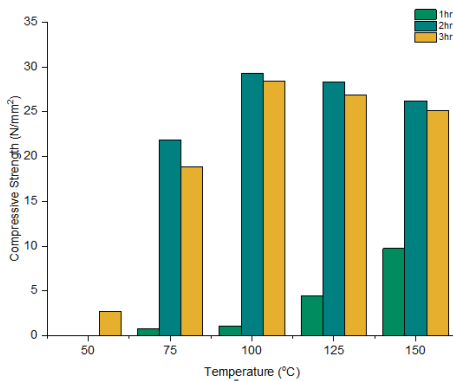


Fig. 2. One day compressive strength of GF with curing temperature and curing time.

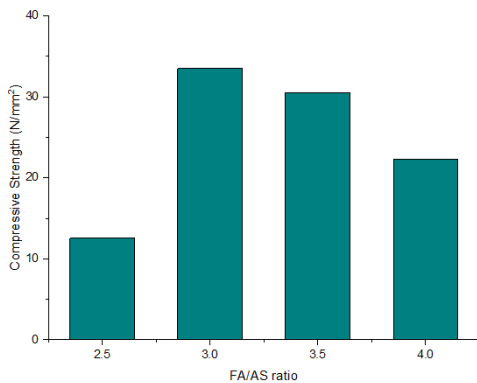


Fig. 3. One day compressive strength of GF with FA/SA ratio.

The one day compressive strength of 10M GF with different FA/AS ratios is shown in Figure 3. The FA/AS ratio was increased by 0.5 at 100°C curing temperature and 2hrs curing time. The maximum strength of GF was observed at the ratio of 3 as 31.47N/mm<sup>2</sup>. The strength decreases beyond FA/AS ratio of 3. The one day CS of GF with different sodium silicate to sodium hydroxide ratios and NaOH molarities is shown in Figure 5. The maximum strength was observed for

Na<sub>2</sub>SiO<sub>3</sub>/NaOH ratio of 1 for every molarity. An increase in CS was observed with increase in molarity due to the increase of Na<sup>+</sup> ions which enhance the geopolymer reaction [29, 31]. Maximum strength was observed in 10M GF cubes. Similar results were reported in [26-28]. When the molarity became more than 10M, a decrease in strength was observed due to the increase in the amount of OH<sup>-</sup> ions which reduce the geopolymer reaction [26].

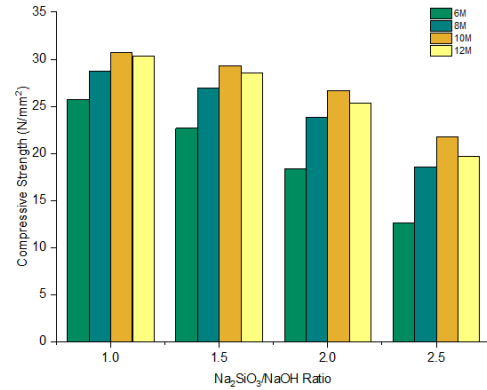


Fig. 4. The one day compressive strength of GF with curing temperature and curing time.

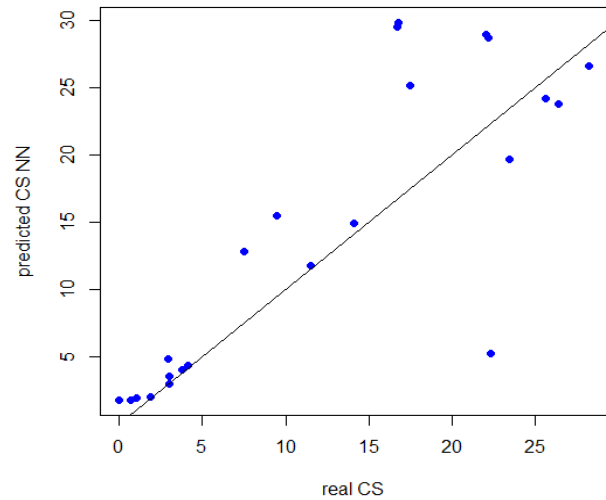


Fig. 5. Comparison between the ANN model predicted data and the experimental data.

B. Modeling Results

The most important step in ANN model development is the ANN architecture determination which suits the real problem. The ANN architecture L-5-4-3-1-1 was finalized after trial and error process. The performance of the ANN model was checked with the performance measures Root Mean Square Error (RMSE) and correction coefficient (R<sup>2</sup>) between the experimental results and the predicted results. They were computed by (4) and (5):

$$RMSE = \sqrt{\frac{\sum (x_i - y_i)^2}{n}} \quad (4)$$

$$R^2 = 1 - \left\{ \frac{\sum (x_i - y_i)^2}{\sum y_i^2} \right\} \quad (5)$$

where  $x_i$  is the target value,  $y_i$  is the predicted value, and  $n$  is the number of test data.

TABLE III. EXPERIMENTAL AND PREDICTED VALUES

Experimental CS (N/mm <sup>2</sup> )	ANN CS (N/mm <sup>2</sup> )
0.71	1.14
7.5	18.7
23.43	18.54
28.25	25.17
17.48	24.15
22.07	26.014
22.21	25.98
2.9	5.06
25.66	26.08
22.32	25.03
26.4	26.08
16.7	24.01
16.8	24.01
3	3.98
1.9	0.234
4.1	4.06
5.9	7.74
13.8	5.3
11.5	6.82
5.2	9.87
1	0
14.1	14.5

Figure 5 represents the ANN model predicted data and the experimental data for the one day compressive strength test. The experimental compressive strength values and the corresponding ANN model predicted compressive strength values are given in Table III. The accuracy of the prediction is indicated by RMSE and  $R^2$ . The RMSE and  $R^2$  obtained values were 4.47 and 0.972 respectively, which show that the ANN is effective in the prediction of the CS of GF.

## V. CONCLUSIONS

This study studies various factors affecting the compressive strength of geopolymer fly ash. The geopolymer fly ash was produced by mixing alkaline solution and fly ash. The factors considered in this study were curing temperature, curing time, fly ash to alkaline solution ratio, sodium silicate to sodium hydroxide ratio, and the molarity of sodium hydroxide. ANNs were employed in this study to predict the compressive strength of GF and the prediction accuracy was validated.

- The selected values of curing temperature were: 50, 75, 100, 125, and 150°C. The maximum compressive strength was observed at 100°C curing temperature.
- The values of curing time were as 1, 2, and 3hr. The maximum compressive strength was observed for 2hr curing time.
- The fly ash to alkaline solution ratio was 2.5, 3, 3.5, and 4. The maximum compressive strength was obtained for ratio equal to 3.

- The Na<sub>2</sub>SiO<sub>3</sub>/NaOH ratio was selected as 1, 1.5, 2, and 2.5. The maximum compressive strength was obtained for the ratio of 1.
- The molarity of NaOH varied as 6, 8, 10, and 12. The maximum compressive strength was obtained for 10M geopolymer fly ash.
- An ANN was developed to predict the compressive strength of GF. The accuracy of the model was evaluated with RMSE and  $R^2$ . The obtained values were 4.47 and 0.972 respectively. These values of RMSE and  $R^2$  confirm that the utilization of ANN for the prediction of the compressive strength of GF is a good choice due to its excellent correlation with the experimental results. This study suggests that ANNs are an effective tool in strength prediction of GF, reducing further the experimental cost and time.
- The geopolymer fly ash with its optimized parameters provides sufficient strength. Hence, it is applicable as a cement replacing material in concrete.

## REFERENCES

- [1] A. M. Fathollahi-Fard, M. Hajiaghahi-Keshteli, and R. Tavakkoli-Moghaddam, "A bi-objective green home health care routing problem," *Journal of Cleaner Production*, vol. 200, pp. 423–443, Nov. 2018, <https://doi.org/10.1016/j.jclepro.2018.07.258>.
- [2] I. Tekin, O. Gencel, A. Gholampour, O. H. Oren, F. Koksall, and T. Ozbakkaloglu, "Recycling zeolitic tuff and marble waste in the production of eco-friendly geopolymer concretes," *Journal of Cleaner Production*, vol. 268, Sep. 2020, Art. no. 122298, <https://doi.org/10.1016/j.jclepro.2020.122298>.
- [3] M. A. Getahun, S. M. Shitote, and Z. C. Abiero Gariy, "Artificial neural network based modelling approach for strength prediction of concrete incorporating agricultural and construction wastes," *Construction and Building Materials*, vol. 190, pp. 517–525, Nov. 2018, <https://doi.org/10.1016/j.conbuildmat.2018.09.097>.
- [4] A. Saand, T. Ali, M. A. Keerio, and D. K. Bangwar, "Experimental Study on the Use of Rice Husk Ash as Partial Cement Replacement in Aerated Concrete," *Engineering, Technology & Applied Science Research*, vol. 9, no. 4, pp. 4534–4537, Aug. 2019, <https://doi.org/10.48084/etasr.2903>.
- [5] N. Bheel, A. W. Abro, I. A. Shar, A. A. Dayo, S. Shaikh, and Z. H. Shaikh, "Use of Rice Husk Ash as Cementitious Material in Concrete," *Engineering, Technology & Applied Science Research*, vol. 9, no. 3, pp. 4209–4212, Jun. 2019, <https://doi.org/10.48084/etasr.2746>.
- [6] S. Khoso, S. A. Abbasi, T. Ali, Z. Soomro, M. T. Naqash, and A. A. Ansari, "The Effect of Water-Binder Ratio and RHA on the Mechanical Performance of Sustainable Concrete," *Engineering, Technology & Applied Science Research*, vol. 12, no. 3, pp. 8520–8524, Jun. 2022, <https://doi.org/10.48084/etasr.4791>.
- [7] A. Mehta and R. Siddique, "Sustainable geopolymer concrete using ground granulated blast furnace slag and rice husk ash: Strength and permeability properties," *Journal of Cleaner Production*, vol. 205, pp. 49–57, Dec. 2018, <https://doi.org/10.1016/j.jclepro.2018.08.313>.
- [8] P. Duxson, A. Fernandez-Jimenez, J. L. Provis, G. C. Lukey, A. Palomo, and J. S. J. van Deventer, "Geopolymer technology: the current state of the art," *Journal of Materials Science*, vol. 42, no. 9, pp. 2917–2933, May 2007, <https://doi.org/10.1007/s10853-006-0637-z>.
- [9] A. Nazari and F. Pacheco Torgal, "Predicting compressive strength of different geopolymers by artificial neural networks," *Ceramics International*, vol. 39, no. 3, pp. 2247–2257, Apr. 2013, <https://doi.org/10.1016/j.ceramint.2012.08.070>.

- [10] J. Davidovits, "High-Alkali Cements for 21st Century Concretes," *Special Publication*, vol. 144, pp. 383–398, Mar. 1994, <https://doi.org/10.14359/4523>.
- [11] J. G. S. Van Jaarsveld, J. S. J. Van Deventer, and L. Lorenzen, "The potential use of geopolymeric materials to immobilise toxic metals: Part I. Theory and applications," *Minerals Engineering*, vol. 10, no. 7, pp. 659–669, Jul. 1997, [https://doi.org/10.1016/S0892-6875\(97\)00046-0](https://doi.org/10.1016/S0892-6875(97)00046-0).
- [12] D. Hardjito, S. E. Wallah, D. M. J. Sumajouw, and B. V. Rangan, "Fly Ash-Based Geopolymer Concrete," *Australian Journal of Structural Engineering*, vol. 6, no. 1, pp. 77–86, Jan. 2005, <https://doi.org/10.1080/13287982.2005.11464946>.
- [13] A. A. Shahmansouri, H. Akbarzadeh Bengar, and S. Ghanbari, "Compressive strength prediction of eco-efficient GGBS-based geopolymer concrete using GEP method," *Journal of Building Engineering*, vol. 31, Sep. 2020, Art. no. 101326, <https://doi.org/10.1016/j.jobbe.2020.101326>.
- [14] Z. H. Duan, S. C. Kou, and C. S. Poon, "Prediction of compressive strength of recycled aggregate concrete using artificial neural networks," *Construction and Building Materials*, vol. 40, pp. 1200–1206, Mar. 2013, <https://doi.org/10.1016/j.conbuildmat.2012.04.063>.
- [15] I. B. Topcu and M. Saridemir, "Prediction of properties of waste AAC aggregate concrete using artificial neural network," *Computational Materials Science*, vol. 41, no. 1, pp. 117–125, Nov. 2007, <https://doi.org/10.1016/j.commatsci.2007.03.010>.
- [16] A. Fouquier, S. Robert, F. Suard, L. Stephan, and A. Jay, "State of the art in building modelling and energy performances prediction: A review," *Renewable and Sustainable Energy Reviews*, vol. 23, pp. 272–288, Jul. 2013, <https://doi.org/10.1016/j.rser.2013.03.004>.
- [17] H. Song *et al.*, "Predicting the compressive strength of concrete with fly ash admixture using machine learning algorithms," *Construction and Building Materials*, vol. 308, Nov. 2021, Art. no. 125021, <https://doi.org/10.1016/j.conbuildmat.2021.125021>.
- [18] K. K. Yaswanth, J. Revathy, and P. Gajalakshmi, "Soft Computing Techniques for the Prediction and Analysis of Compressive Strength of Alkali-Activated Alumino-Silicate Based Strain-Hardening Geopolymer Composites," *Silicon*, vol. 14, no. 5, pp. 1985–2008, Apr. 2022, <https://doi.org/10.1007/s12633-021-00988-7>.
- [19] D. Tsamatsoulis, "Prediction of Cement Compressive Strength by Combining Dynamic Models of Neural Networks," *Chemical and Biochemical Engineering Quarterly*, vol. 35, no. 3, pp. 295–318, Oct. 2021, <https://doi.org/10.15255/CABEQ.2021.1952>.
- [20] H. Chen, C. Qian, C. Liang, and W. Kang, "An approach for predicting the compressive strength of cement-based materials exposed to sulfate attack," *PLOS ONE*, vol. 13, no. 1, Jan. 2018, Art. no. e0191370, <https://doi.org/10.1371/journal.pone.0191370>.
- [21] M. M. Yadollahi, A. Benli, and R. Demirboga, "Prediction of compressive strength of geopolymer composites using an artificial neural network," *Energy Materials*, vol. 10, no. 3, pp. 453–458, Sep. 2015, <https://doi.org/10.1179/1433075X15Y.0000000020>.
- [22] *ASTM C618-19(2008), Standard Specification for Coal Fly Ash and Raw or Calcined Natural Pozzolan for Use in Concrete*. West Conshohocken, PA, USA: ASTM International, 2008.
- [23] *IS 1727 (1967), Method of test for pozzolanic materials*. New Delhi, India: Bureau of Indian Standards, 1967.
- [24] A. Azadeh, J. Seif, M. Sheikhalishahi, and M. Yazdani, "An integrated support vector regression–imperialist competitive algorithm for reliability estimation of a shearing machine," *International Journal of Computer Integrated Manufacturing*, vol. 29, no. 1, pp. 16–24, Jan. 2016, <https://doi.org/10.1080/0951192X.2014.1002810>.
- [25] *ASTM C109/C109M-20(2011), Standard Test Method For Compressive Strength Of Hydraulic Cement Mortars (Using 2-In. Or [50-Mm] Cube Specimens)*. West Conshohocken, PA, USA: ASTM International, 2011.
- [26] S. Parvathy S, A. K. Sharma, and K. B. Anand, "Comparative study on synthesis and properties of geopolymer fine aggregate from fly ashes," *Construction and Building Materials*, vol. 198, pp. 359–367, Feb. 2019, <https://doi.org/10.1016/j.conbuildmat.2018.11.231>.
- [27] S. M. Rao and I. P. Acharya, "Synthesis and Characterization of Fly Ash Geopolymer Sand," *Journal of Materials in Civil Engineering*, vol. 26, no. 5, pp. 912–917, May 2014, [https://doi.org/10.1061/\(ASCE\)MT.1943-5533.0000880](https://doi.org/10.1061/(ASCE)MT.1943-5533.0000880).
- [28] U. S. Agrawal, S. P. Wanjari, and D. N. Naresh, "Characteristic study of geopolymer fly ash sand as a replacement to natural river sand," *Construction and Building Materials*, vol. 150, pp. 681–688, Sep. 2017, <https://doi.org/10.1016/j.conbuildmat.2017.06.029>.
- [29] P. Chindapasirt, C. Jaturapitakkul, W. Chalee, and U. Rattanasak, "Comparative study on the characteristics of fly ash and bottom ash geopolymers," *Waste Management*, vol. 29, no. 2, pp. 539–543, Feb. 2009, <https://doi.org/10.1016/j.wasman.2008.06.023>.
- [30] A. Sathonsaowaphak, P. Chindapasirt, and K. Pimraksa, "Workability and strength of lignite bottom ash geopolymer mortar," *Journal of Hazardous Materials*, vol. 168, no. 1, pp. 44–50, Aug. 2009, <https://doi.org/10.1016/j.jhazmat.2009.01.120>.